Available online at www.sciencedirect.com
SCIENCE DIRECT®
Journal of Molecular Catalysis A: Chemical 223 (2004) 67–74
JOURNAL OF MOLECULAR CATALYSIS A: CHEMICAL
www.elsevier.com/locate/molcata

Supported sulfated zirconia catalysts and their properties

Hillary A. Prescott, Martin Wloka, Erhard Kemnitz*

Institut für Chemie, Humboldt Universität zu Berlin, Brook-Taylor-Str. 2, 12489 Berlin, Germany

Received 8 February 2003; received in revised form 27 October 2003; accepted 1 November 2003
Available online 15 September 2004

Abstract

Sulfated zirconia (SZ), SO_4/ZrO_2, was supported by SiO_2, γ-Al_2O_3, and K-10. Aspects of preparation, such as ZrO_2 precursor, sulfur contents, sulfating agent, and calcination conditions, were studied. The pure supports and catalysts were characterized with XRD, BET, FTIR photoacoustic spectroscopy (pyridine adsorption), NH_3-TPD, and tested for the benzoylation of anisole with benzoyl chloride. The support strongly affects the catalytic activity; SZ supported by K-10 achieved catalytic yields higher than that of bulk SZ.

Keywords: Supported sulfated zirconia; Acidity; Properties

1. Introduction

Sulfated zirconia (SZ) has been of interest for some time as a catalyst in the acylation of aromatics [1], a reaction normally catalyzed by superacids or Lewis acids [2]. Sulfated zirconia provides a catalyst that is solid and easier-to-handle than the corrosive, liquid acids usually used. This environmentally friendly catalyst is an alternative to the stoichiometric amounts of Lewis acids normally needed to "catalyze" this reaction, which result in high amounts of byproducts. Until now, most research has been done on bulk SZ prepared by the sulfation of precipitated zirconium hydroxide with or without metallate promotion [3].

To reduce costs, improve surface properties, and find a mechanically stable form of sulfated zirconia suitable for large-scale industrial processes, the possibility of supporting SZ is being studied. Common supports for SZ found in the literature are SiO_2 [4–6], γ-Al_2O_3 [5,6], and the zeolite, FSM [7]. Pt promotion of sulfated zirconia supported by SiO_2 or γ-Al_2O_3 has also been examined [8]. The catalytic activity of these supported catalysts has been studied for the following reactions: *n*-octane hydroisomerization [8], etherification [4], hexane conversion [5], 1-butene isomerization [7], and *n*-butane isomerization [6]. In [7], the FSM-supported SZ (SZ/FSM) catalyst was catalytically inactive for the benzoylation of toluene with both benzoyl chloride and benzoic acid anhydride. This was attributed to the low acidity of the supported catalyst, not the pore size [7]. However, results for Mukaiyama aldol condensation were comparable for SZ and SZ/FSM indicating a sufficient amount of strong acid sites in the supported catalyst for this reaction [7].

We studied the preparation, physical surface properties, surface acidity, and catalytic activity of SZ catalysts supported by SiO_2, γ-Al_2O_3, and K-10. The catalytic activity was screened by the benzoylation of anisole with benzoyl chloride. The pure supports, SiO_2, γ-Al_2O_3, and K-10, and the supported SZ catalysts were examined. Aspects of preparation, i.e., ZrO_2 precursor and consequent synthesis, sulfur contents, sulfating agent, were varied and are discussed. In this paper, we report on the properties of *selected* supported SZ catalysts and their catalytic activities for the benzoylation of anisole.

2. Experimental

2.1. Sample preparation

Supported SZ catalysts were prepared by varying such factors as the ZrO_2 precursor, the sulfating agent and sulfur

* Corresponding author. Tel.: +49 30 2093 7555; fax: +49 30 2093 7277.
E-mail address: erhard.kemnitz@chemie.hu-berlin.de (E. Kemnitz).

1381-1169/$ – see front matter © 2004 Elsevier B.V. All rights reserved.
doi:10.1016/j.molcata.2003.11.037

contents, the support, and calcination conditions. An overview of the preparation is given in Table 1. Sample notation indicates the support (Al for Al_2O_3, Si for SiO_2, and K for K-10), the ZrO_2 precursor (zirconyl chloride was used unless otherwise indicated with S for zirconium sulfate or N for zirconium nitrate), and when applicable, oven drying (od) or freeze drying (fd) procedures, respectively, for SZ/Al samples; the sulfur contents is given in parenthesis at the end of the sample code, for example, SZ/Al-fd(2.2) is a freeze-dried, Al_2O_3-supported SZ with an experimental sulfur contents of 2.3 wt.% S and zirconyl chloride as the precursor, or SZ/Si-1(2.3), a SiO_2-supported SZ sample with 2.3 wt.% S prepared from the ZrO_2 precursor, zirconyl chloride. In the case of the chloride or nitrate and complete evaporation of the solvent, the theoretical wt.% ZrO_2 was calculated from the amount of the ZrO_2 precursor used during synthesis. When the excess precursor solution was filtered off, the wt.% of ZrO_2 was calculated from the volume of precursor solution adsorbed by the support. In the case of $Zr(SO_4)_2{\cdot}2H_2O$, the wt.% ZrO_2 was calculated from the elemental sulfur contents of the sample prior to calcination.

2.2. Variation of support

The γ-Al_2O_3-supported catalysts, SZ/Al-od(2.2) and SZ/Al-fd(2.2), were prepared by impregnation of γ-Al_2O_3 (Leuna Werk) with an aqueous solution of 5 M $ZrOCl_2{\cdot}8H_2O$ (Fluka, 99%) and 2.2 M $(NH_4)_2SO_4$ (Isocommerz, p.a.). The soaked support was then exposed to flowing NH_3 gas. The samples were then oven-dried at 100 °C [SZ/Al-od(2.2)] or freeze-dried [SZ/Al-fd(2.2)] followed by calcination at 550 °C in Ar.

The preparation of SZ/Si-1(2.3), a SiO_2-supported catalyst, involved soaking the SiO_2 support (Alfa Aesar, wide pore, 150 Å) in an aqueous 0.6 M solution of $ZrOCl_2{\cdot}8H_2O$. After complete evaporation, the sample was freeze-dried. NH_3 gas was then flowed over the freeze-dried sample for 1 h prior to further drying at 100 °C. The sample was then sulfated by impregnation with 1 M H_2SO_4 and calcined at 550 °C in Ar.

The Montmorillonite K-10 (Aldrich) supported catalysts, SZ/K-2(2.0) and -2a(3.9), were synthesized similarly to SZ/Si-1(2.3). Instead of freeze drying, the excess aqueous 1 M $ZrOCl_2{\cdot}8H_2O$ solution was filtered off after

Table 1
Preparation details and sample codes of the supported SZ samples

Sample code	ZrO_2 precursor (wt.%)	Support	Sulfating agent[a]	Sulfur contents (theor./exptl., wt.%)	Calcination temperature (°C)/atm
γ-Al_2O_3					
SZ/Al-od(2.2)	Cl, 28	γ-Al_2O_3	$(NH_4)_2SO_4$	4.3/2.2	550/Ar(od)[b]
SZ/Al-fd(2.2)	Cl, 28	γ-Al_2O_3	$(NH_4)_2SO_4$	4.3/2.2	550/Ar(fd)[b]
SiO_2					
SZ/Si-1(2.3)	Cl, 17[c]	SiO_2	H_2SO_4	3.0/2.3	550/Ar
SZ/Si-N(2.6)	N, 20[c]	SiO_2	H_2SO_4	3.0/2.6	600/air
SZ/Si-S(0.7)	S, 12[c,d]	SiO_2	n.a.	5.9/0.7	700/air
K-10					
SZ/K-S(1.5)	S	K-10	n.a.	–/1.5	700/air
SZ/K-Sa(2.0)	S, 12[c]	K-10	n.a.	2.8/2.0	700/air
SZ/K-Sb(1.7)	S, 12[c]	K-10	n.a.	–/1.7	700/air
SZ/K-2(2.0)	Cl, 17	K-10	H_2SO_4	5.0/2.0	600/air
SZ/K-2a(3.9)	Cl, 17	K-10	H_2SO_4	5.0/3.9	600/air
Series samples					
SZ/Al-2a(1.0)	Cl, 17	γ-Al_2O_3	H_2SO_4	1.0/1.0	600/air
SZ/Al-2b(2.1)	Cl, 17	γ-Al_2O_3	H_2SO_4	2.0/2.1	600/air
SZ/Al-2c(2.9)	Cl, 17	γ-Al_2O_3	H_2SO_4	3.0/2.9	600/air
SZ/Al-2d(3.3)	Cl, 17	γ-Al_2O_3	H_2SO_4	4.0/3.3	600/air
SZ/Al-2e(3.4)	Cl, 17	γ-Al_2O_3	H_2SO_4	5.0/3.4	600/air
SZ/Si-2a(1.2)	Cl, 17[c]	SiO_2	H_2SO_4	1.0/1.2	600/Ar
SZ/Si-2b(2.0)	Cl, 17	SiO_2	H_2SO_4	2.0/2.0	600/Ar
SZ/Si-2b1(1.9)	Cl, 17	SiO_2	H_2SO_4	2.0/1.9	600/Ar
SZ/Si-2c(2.7)	Cl, 17[c]	SiO_2	H_2SO_4	3.0/2.7	600/Ar
SZ/Si-2d(3.0)	Cl, 17	SiO_2	H_2SO_4	4.0/3.0	600/Ar
SZ/Si-2e(3.2)	Cl, 17[c]	SiO_2	H_2SO_4	5.0/3.2	600/Ar

[a] 1 M H_2SO_4 or $(NH_4)_2SO_4$ (aq).
[b] od: oven-dried, fd: freeze-dried.
[c] Confirmed by AES-ICP measurements; Cl, N, and S indicate the ZrO_2 precursor: chloride, nitrate, or sulfate, respectively.
[d] Calculated from wt.% S precalcination.

impregnation of the support. The sample was then exposed to NH_3, sulfated with 1 M H_2SO_4, and dried at 60 °C followed by calcination at 600 °C in air.

2.3. Variation of sulfur contents

The influence of the sulfur contents on the catalytic activity was studied with a series of SZ/Si-2 and SZ/Al-2 samples (Table 1). These samples were all prepared with respective amounts of $ZrOCl_2{\cdot}8H_2O$ and 1 M H_2SO_4 to yield SZ (17 wt.% ZrO_2 and 1–5 wt.% S) on SiO_2 or γ-Al_2O_3. The steps of synthesis were identical to that of the SZ/K-2(2.0) samples.

2.4. Variation of ZrO_2 precursor

In the case of SZ/Si-N(2.6), the support, SiO_2, was soaked in an aqueous 0.7 M solution of zirconium nitrate (Reakhim, pure). The excess water was evaporated off and the sample was dried overnight. The sample was then precalcined at 300 °C to decompose the nitrate. Final calcination was carried out under the same conditions described for the SZ/Si-2 samples after impregnation with 1 M H_2SO_4.

Zirconium sulfate hydrate (Aldrich, 99.99%) was also used as a ZrO_2 precursor. The samples, SZ/Si-S, SZ/K-S(1.5), -Sa(2.0), and -Sb(1.7), and were prepared by simply soaking the supports, K-10 and SiO_2, respectively, in an aqueous 1 M solution of zirconium sulfate hydrate. The samples were then calcined at 700 °C in air after drying for 12 h at 120 °C.

2.5. Catalyst characterization

The concentrations of the elements, Si and Zr, in SZ/Si samples were measured with a Unichem 701 ICP atomic emission spectrometer (ICP-AES), which was calibrated before each use with standard solutions. The ICP-AES results of the samples measured (indicated by * in Table 1) show that theoretical and experimental loadings of ZrO_2 agree to within 2%, i.e., 20 and 22 wt.% ZrO_2, respectively, for SZ/Si-N(2.6).

The sulfur contents of the samples were determined by standard elemental analysis with a Leco CHNS-932 analyzer and VTF 900 extension.

The XRD patterns of the supports and supported catalysts were recorded on a RD 7 Seiffert-FPM diffractometer (Cu Kα radiation, Ni-filter, 2θ = 5–64°, 0.050 step, 5 s/step).

Low temperature nitrogen adsorption experiments were carried out on a Micromeritics ASAP 2000 at 77 K with N_2 to determine the specific BET surface areas (S_{BET}), the pore dimensions (V_P and D_P), and pore size distributions.

The total concentration of acid sites of the sample was measured quantitatively by NH_3 temperature programmed desorption (NH_3-TPD). NH_3 was adsorbed in excess at 120 °C on the sample in flowing Ar after sample pretreatment at 500 °C for 1 h under Ar. After flushing the sample with Ar, NH_3-TPD was measured between 80 and 500 °C at 10 °C/min holding at 80 °C for 1 min and 500 °C for 30 min. NH_3 desorption was detected by monitoring the NH_3 band at 930 ± 5 cm^{-1} with a Perkin-Elmer FTIR system 2000 spectrometer. The total NH_3 desorbed was then quantitatively determined by reaction with excess sulfuric acid and back titration with NaOH.

The type of acid sites (Lewis, L, or Brønsted, B) present in the supported catalysts was studied with FTIR photoacoustic spectroscopy (FTIR-PAS) of chemisorbed pyridine adsorbate complexes (PACs). The measurements were carried out before and after pyridine adsorption between 400 and 4000 cm^{-1} in a MTEC 300-photoacoustic cell on the IR spectrometer described above. The sample (pretreated at 150 °C for 30 min under Ar) was exposed to pyridine (2× 30 μL) at 150 °C with Ar flushing in between for 15 min. The normalization of the spectra is described in [1].

Benzoylation of anisole with benzoyl chloride was carried out at 60 °C for 3 h under flowing N_2 in a three-neck, round bottom flask with reflux condenser. Benzoyl chloride (373 mg, 2.65 mmol, Fluka, 99.5%), *n*-tridecane (GC-internal standard, approx. 60 mg, 0.3 mmol, Fluka, 99.5%), and anisole (11.7 g, 108 mmol, Fluka, 99%) were stirred together and heated to 60 °C. The catalyst (200 mg) was then added to the mixture after pretreatment at 200 °C for 1 h.

Samples (0.3 μL) of the reaction mixture were taken before and after reaction and analyzed gas chromatographically by a Varian 3400 GC with a wide bore column DB5 (J & W Scientific, USA) (length 15 m, inner diameter 0.53 mm) with FID: 340 °C, injector: 320 °C, temperature program: 120 °C (3 min) to 220 °C (2 min) at a heating rate of 20 °C/min. Catalytic results were based on the *conversion* of benzoyl chloride, the total *yield* of 2- and 4-methoxybenzophenone, and the *selectivity* of these products.

3. Results and discussion

3.1. XRD and physical surface properties

The XRD patterns of the supports and supported catalysts in Fig. 1a–f show only broad, weak peaks for amorphous phases. The patterns of SZ/K-2(2.0) and pure K-10 (Fig. 1g and h, respectively), on the other hand, do show some phase crystallinity and sharper peaks for K-10.

In the pattern of γ-Al_2O_3 (Fig. 1d), broad peaks are observed at about 40° and 45°, which decrease in intensity (45°) or disappear entirely (40°) when the support is loaded. Damyanova et al. attributed this to the interaction of ZrO_2 with the support and the covering of alumina with ZrO_2 crystallites [9]. Weak peaks confirm the presence of these crystallites at 30° and 50° (Fig. 1a and b) for ZrO_2 [10]. No such peaks were observed in the pattern of SZ/Al-2d(3.3) (Fig. 1c) due to its lower ZrO_2 loading of 17%. Nonetheless, the characteristic peaks for γ-Al_2O_3 decrease in intensity for this sample probably based on partial reaction of γ-Al_2O_3 with the sulfating agent, H_2SO_4.

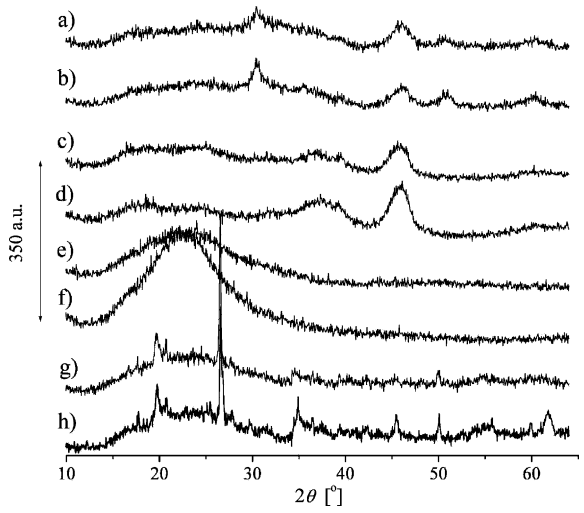

Fig. 1. XRD patterns of (a) SZ/Al-od(2.2), (b) SZ/Al-fd(2.2), (c) SZ/Al-2d(3.3), (d) the support, γ-Al_2O_3, (e) SZ/Si-1(2.3), (f) the support (SiO_2), (g) SZ/K-2(2.0) and (h) the support, K-10.

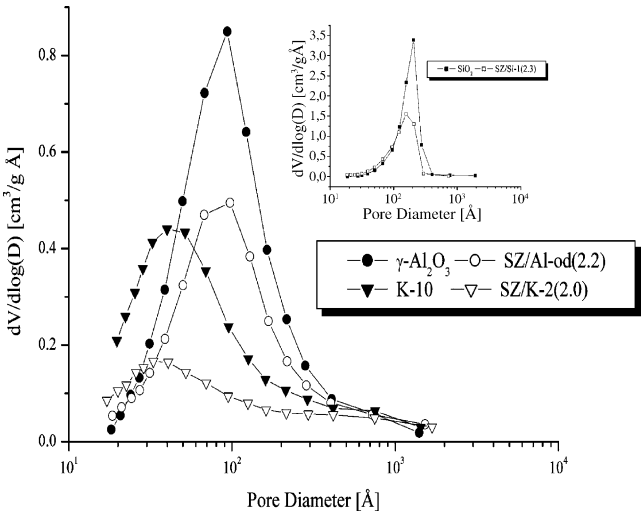

Fig. 2. BJH adsorption pore size distributions of the indicated samples. Open symbols indicate the support; closed symbols indicate the loaded support.

The XRD pattern of the SiO_2 support (Fig. 1f) shows a broad peak between 15° and 30°, which broadens and losses intensity after SZ loading (Fig. 1e). No peaks are observed for tetragonal ZrO_2, which indicates a good dispersion of the lower loading of the ZrO_2 phase (17 wt.% instead of 28 wt.%). The samples, SZ/K10-2(2.0) and K-10, show a higher crystallinity than the others, yet similar to the γ-Al_2O_3-supported samples, the peaks of K-10 (Fig. 1h) decrease in intensity significantly, when K-10 is modified with SZ (Fig. 1g). Again, no peaks were observed for the ZrO_2 phase with a loading less than 20 wt.%.

The surface area (S_{BET}), total pore volume (V_P), and average pore diameter (D_P) of the SiO_2, γ-Al_2O_3, and K-10 supports and selected supported catalysts are given in Table 2. The surface area, pore volume, and pore diameter of the SiO_2 and γ-Al_2O_3-supported catalysts are, as expected, much higher than that of the bulk catalyst [11], but the porosity is slightly lower than that of the SZ aerogel [12]. The K-10-supported catalysts have much lower surface areas and pore volumes than that of pure K-10 and the SiO_2 and γ-Al_2O_3-supported catalysts. The average pore diameters of the SZ/K samples are 65 and 71 Å, both higher than that of the K-10 support.

The decrease in S_{BET} and V_P of the loaded supports (Table 2) indicates a complete filling of some of the pores by the SZ component preventing N_2 adsorption in the filled pores [13]. The pore size distribution curves (Fig. 2) confirm this by showing an intensity decrease without a pore diameter shift of the maxima at 40, 100, and 110 Å for K-10, γ-Al_2O_3, and SiO_2, respectively. In [6], the pore size distribution curves did show a shift to lower pore diameters when the support was loaded, indicating, in comparison to here, not only a complete filling of some of the pores, but also partial filling of the other pores.

3.2. Surface acid properties

The surface acid properties of the supports and selected supported SZ samples were characterized with NH_3-TPD and FTIR photoacoustic spectroscopy of pyridine adsorbate complexes (PACs) on the surface of the catalysts. The FTIR photoacoustic spectra and NH_3 profiles from the NH_3-TPD measurements of selected samples are compared in Figs. 3 and 4. The semiquantitative intensities of the bands at approx. 1450, 1490, and 1550 cm^{-1} in the IR spectra and the total concentration and density of acid sites measured by the amount of NH_3 desorbed during NH_3-TPD are all given in Table 2.

In Fig. 3a, the spectra of PACs on the surface of the supports show that SiO_2 has no surface acid sites (no bands observed), whereas a weak band at about 1450 cm^{-1} indicates the presence of Lewis acid sites in γ-Al_2O_3. The support, K-10, in comparison, has both Lewis and Brønsted acid sites; all three bands are present in the spectrum (Fig. 3a).

Loading of SZ on to SiO_2 and γ-Al_2O_3 (Fig. 3b) increases the number of Lewis acid sites indicated by strong bands at about 1450 and 1490 cm^{-1} [SZ/Si-1(2.3) and SZ/Al-od(2.2)]. In the case of SZ/Si-1(2.3), the band at 1450 cm^{-1} is shifted to 1446 cm^{-1} for weaker acid sites. Brønsted acid sites are also indicated in this sample by the weak, broad band at about 1550 cm^{-1}. SZ/Al-od(2.2) has few or no Brønsted acid sites and only a few Lewis acid sites (Fig. 3b and Table 2). The loading of ZrO_2 on the Al_2O_3 and SiO_2 supports described in [9] generated new Lewis and weaker Brønsted acid sites in ZrO_2/SiO_2 similar to the results presented here. In comparison, the increased loading of ZrO_2 on Al_2O_3 reduced the number of total and strong Lewis acid sites [9]. This effect was not studied here. Nonetheless, it seems that little or no change in acidity is observed, when the supported ZrO_2 phase is sulfated in contrast to the sulfation of bulk ZrO_2 [1]. Acidic strength measurements on SZ/MCM-41 and SZ presented in

Table 2
Sulfur contents and surface properties of selected samples

Sample	S_{BET} (m^2/g)	V_P (cm^3/g)	D_P (Å)	Total concentration/density of acid sites (NH_3-TPD)		Relative band intensities		
				μmol/g	μmol/m^2	L (1450 ± 5 cm^{-1})	L/B (1490 ± 5 cm^{-1})	B (1550 ± 5 cm^{-1})
γ-Al_2O_3	241	0.57	94	241	1.0		n.a.	
SZ/Al-od(2.2)	178	0.39	89	170	0.95	12.1	4.0/3.2	n.a.
SZ/Al-fd(2.2)	169	0.40	96	n.d.	n.d.		n.d.	
SiO_2	280	1.10	158	3	0.01		n.a.	
SZ/Si-1(2.3)	239	0.71	119	359	1.50	13.1	4.4/5.1	1.8
SZ/Si-N(2.6)	203	0.71	138	274	1.35	1.3	0.4/4.3	3.1
SZ/Si-2a(1.2)	245	0.78	124	390	1.59	6.2	2.1/4.1	3.0
SZ/Si-2e(3.2)	209	0.69	133	308	1.47	2.5	0.8/6.2	2.9
K-10	279	0.38	55	288	1.03	4.9	11.9/10.2	4.5
SZ/K-S(1.5)		n.d.		196	–		n.d.	
SZ/K-Sa(2.0)	78	0.14	71	146	1.87		3.52	1.3
SZ/K-2(2.0)	116	0.14	65	n.d.	n.d.		n.d.	
SZ/K-2a(3.9)		n.d.		136	n.d.	2.6	0.85/6.2	∼2.8

L, Lewis acid site; B, Brønsted acid site; n.d., not determined; n.a., not applicable.

[13] showed that the supported SZ phase had a lower acidic strength than the bulk material, but that it was ascribed as "superacidic".

In general, the band at 1490 cm^{-1} can be assigned to PACs bonded to both Brønsted and Lewis acid sites. When Lewis acid sites are exclusively present in the sample, the 1490 cm^{-1} band intensity is one-third that of the 1450 cm^{-1} band. In the spectra of SZ/K-2a(3.9) (Fig. 3b), the band at 1490 cm^{-1} is comparable in intensity to that in the SZ/Si-1(2.3) and SZ/Al-od(2.2) spectra, yet the band observed at 1450 cm^{-1} is much weaker in intensity and shifted to 1446 cm^{-1}. Therefore, the intensity of the band at 1490 cm^{-1} can be attributed to Brønsted acid sites in SZ/K-2a(3.9) also indicated by a broad band between 1520 and 1560 cm^{-1}. These Brønsted acid sites could explain the improved catalytic yields of the SZ/K catalysts (Table 3) and originate directly from the support. The presence of Brønsted acid sites in K-10 and a decrease in these sites with SZ loading [14] [compare Fig. 3a and b: K-10 and SZ/K-2a(3.9)] is also indicated.

The TPD measurements (Table 2 and Fig. 4a–c) show similar results. Here, the total concentration of acid sites of K-10 decreases significantly from 288 to <200 μmol/g, when K-10 is loaded with SZ. The corresponding surface density of acid sites, however, increases from 1.03 to 1.87 μmol/m^2. The total number of acid sites of SZ/K-Sa(2.0) and K-10 correlate with their PAC IR band intensity values (Table 2). Pure K-10 also exhibits delayed desorption during isothermal conditions at 500 °C, which was reduced when the support was loaded (compare Fig. 4a and b: dashed lines). NH_3-TPD also confirms the lack of acid sites in SiO_2 by an almost negligible amount of NH_3 desorbed (3 μmol/g, Table 2) and no significant maximum in the NH_3 profile (Fig. 4a: dotted line).

In the case of γ-Al_2O_3, it is more complicated. NH_3 is desorbed from γ-Al_2O_3 from about 175 to 500 °C. Desorption continues on at isothermal conditions (500 °C for about 30 min), but only a small amount of Lewis acid sites are present in γ-Al_2O_3 (Fig. 3a). Thus, the NH_3 gas adsorption of γ-Al_2O_3 seems to be independent of its acid sites, which is also the case for CaO [15].

Interestingly enough, the SZ/Si samples had the highest concentrations of acid sites (279–390 μmol/g, Table 2 and Fig. 4b). This is a direct result of the SZ loading and can be attributed to Lewis acid sites. The other samples, SZ/Al and SZ/K, have lower concentrations of acid sites (<300 μmol/g) and different NH_3 profiles. The profiles of SZ/Si and SZ/Al

Table 3
Catalytic activities of samples including the series samples, SZ/Si-2 and SZ/Al-2 for the benzoylation of anisole at 60 °C for 3 h

Sample	Conversion (%)	Selectivity (%)	Yield (%)
γ-Al_2O_3		n.d.	
SZ/Al-od(2.2)	10.0	67.6	7.0
SZ/Al-fd(2.2)	14.1	39.6	5.6
SiO_2		n.d.	
SZ/Si-1(2.3)	12.1	65.3	7.9
SZ/Si-N(2.6)	28.9	32.5	7.1
SZ/Si-S(0.7)	16.5	58.0	9.5
K-10	35	60.9	21.3
SZ/K-S(1.5)	20.9	75.1	15.7
SZ/K-Sa(2.0)	23.5	38.8	9.1
SZ/K-Sb(1.7)	18.6	64.6	12.0
SZ/K-2(2.0)	37.2	78.3	28.4
SZ/K-2a(3.9)	30.3	80.9	24.5
Series samples			
SZ/Al-2a(1.0)		n.d.	
SZ/Al-2b(2.1)		n.d.	
SZ/Al-2c(2.9)	14.6	7.8	1.1
SZ/Al-2d(3.3)	17.6	2.1	0.4
SZ/Al-2e(3.4)		n.d.	
SZ/Si-2a(1.2)	23.2	17.3	4.0
SZ/Si-2b(2.0)	18.8	39.9	7.5
SZ/Si-2b1(1.9)	15.5	36.5	6.0
SZ/Si-2c(2.7)	18.1	33.3	6.0
SZ/Si-2d(3.0)	18.6	33.8	6.3
SZ/Si-2e(3.2)	15.8	47.4	7.5

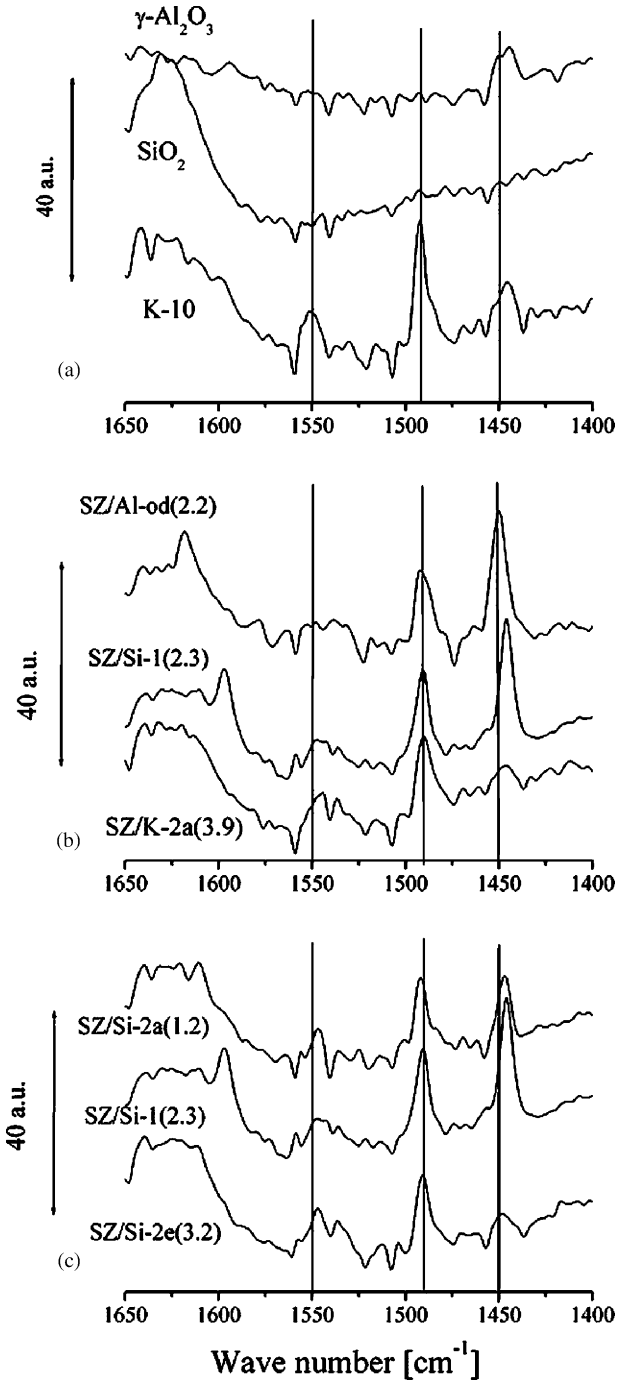

Fig. 3. FTIR photoacoustic spectra of pyridine adsorbate complexes on (a) the pure supports, (b) supported SZ samples and (c) samples with different S contents.

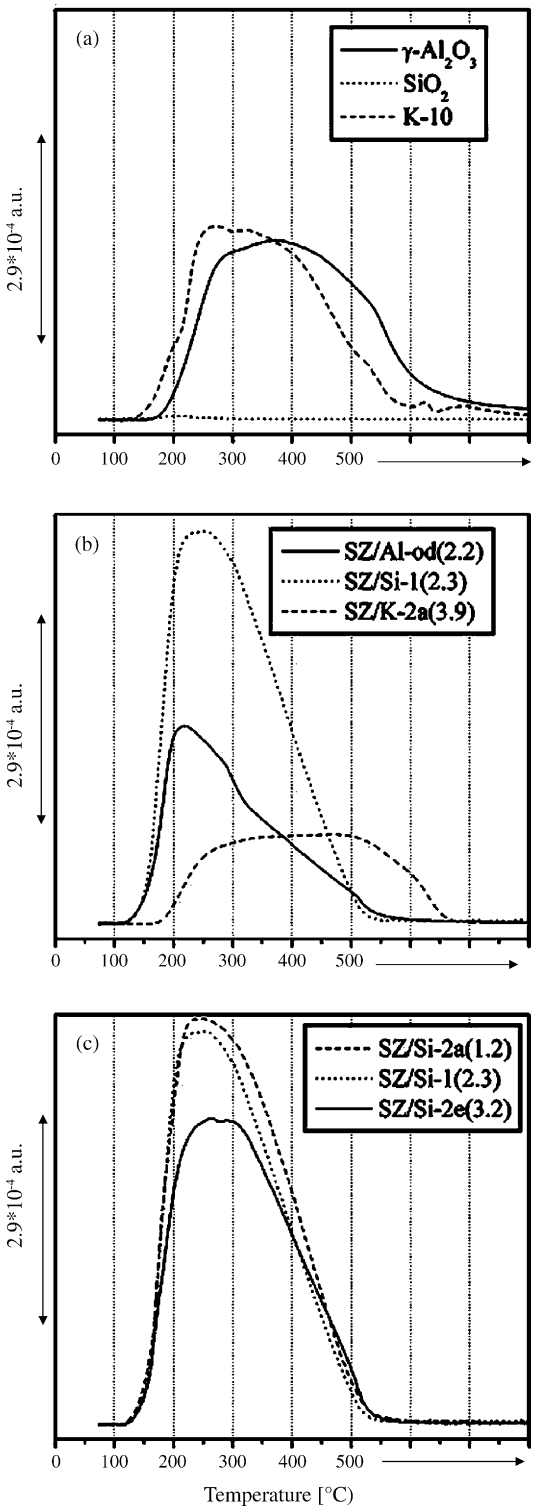

Fig. 4. NH_3-TPD profiles of (a) the pure supports, (b) supported SZ samples and (c) samples with different S contents.

have rounded maxima between 200 and 300 °C, with an abrupt decrease at 300 °C for SZ/Al, yet the desorption of NH_3 on SZ/Al above 300 °C is much more gradual than that of SZ/Si, which has predominantly weaker Lewis acid sites. In the case of SZ/K, desorption of NH_3 begins at a slightly higher temperature (about 175 °C). A very broad, flat maximum is observed between 250 and 375 °C indicating an even distribution of moderate acid sites in this temperature range. The shape of the NH_3-TPD profile for SZ/K-2a(3.9) is very similar to that of the K-10 support.

In the case of SZ/Si, the sulfur contents also influences the total concentration of acid sites of the samples, but not their strengths. Variations in the FTIR photoacoustic spectra

of PACs (Fig. 3c) are also observed for the SZ/Si samples: SZ/Si-2a(1.2), SZ/Si-1(2.3), and SZ/Si-2e(3.2). Interestingly enough, the intensity of the band at about 1490 cm^{-1} remains almost constant, independent of the sulfur contents. On the other hand, drastic changes are observed in the amount of Lewis acid sites (band at about 1450 cm^{-1}). SZ/Si-1(2.3) has the highest amount of Lewis acid sites. Sulfur contents of 1.2 and 3.2 wt.% result in a lower amount of Lewis acid sites. The bands at around 1550 cm^{-1} for Brønsted acid sites are broad and difficult to interpret; however, a slight trend to higher intensities with sulfur contents can be seen (Table 2 and Fig. 3c). This could explain why only slight variations are observed in the catalytic yields and no direct correlation with acidity can be made.

TPD measurements show a direct correlation of the total concentration of acid sites and their surface density with S contents (Table 2): 390/1.59 for SZ/Si-2a(1.2), 359/1.50 for SZ/Si-1(2.3), and 308 μmol/g/1.47 μmol/m^2 for SZ/Si-2e(3.2). The number of acid sites and their density is indirectly proportional to S contents. Fig. 4c shows similar profiles for all three samples with desorption starting at about 125 °C. The profiles of the samples with 2.3 and 1.2 wt.% S are almost identical except for the slightly higher intensity of the curve of the sample with 1.2 wt.% S and a slight shift of the maximum to higher temperatures. On the other hand, the profile of SZ/SiO_2-2e (3.2 wt.% S) is much lower in intensity, has a broader maximum between 200 and 350 °C, and desorbs NH_3 more gradually between 300 and 500 °C than the other two samples. This indicates the presence of stronger acid sites.

3.3. Catalysis and synthesis

Catalytic results of the benzoylation of anisole with benzoyl chloride are presented in Table 3. The supported SZ samples vary from being inactive to having higher yields than that of bulk SZ (catalytic yield: 21% [11]) in the benzoylation of anisole.

3.4. Support and preparation methods

The support seems to have a significant effect on the activity of the supported SZ sample. Catalytic yields of SZ/Al samples are very low between 0 and 7.0%. The freeze-dried sample, SZ/Al-fd(2.2), has a catalytic activity lower than that of the oven-dried sample, SZ/Al-od(2.2) (Table 3); therefore, most of the samples were simply oven-dried. SZ/Si samples achieve yields of 4.0–10.0%. The highest catalytic activities, however, are observed for SZ/K samples, which are, to some extent, even higher than that of bulk SZ (>21%). The improved activity of the SZ/K samples compared with that of SZ/Si and SZ/Al could be attributed to the added acid sites of the K-10 support observed by FTIR-PAS and NH_3-TPD. Another indication of this is the activity of pure K-10 in the benzoylation reaction with a catalytic yield of 21.3%.

3.5. ZrO_2 precursor

Samples were prepared with zirconium oxychloride octahydrate, zirconium nitrate, and zirconium sulfate hydrate (Table 1). Calcination temperatures of 550 or 600 °C and atmospheres of Ar or air for samples prepared from the nitrate or chloride precursors were varied (Table 1), but a strong influence on catalytic activity could not be established here. The calcination temperature (700 °C) of the samples prepared from the sulfate precursor was optimized to yield a sulfur content of around 2 wt.% S [Table 1: SZ/K-Sa(2.0) and -Sb(1.7)].

Use of the sulfate produced a more active SZ/Si phase (catalytic yield: 9.5%) than that of the chloride or nitrate (catalytic yield: 7.0–8.0%). Interestingly enough, when K-10 is the support, just the opposite is true. Here, the activity of the catalyst prepared from the sulfate was much lower than that synthesized from chloride: 15.7% [SZ/K-S(1.5)] compared to 28.4% for [SZ/K-2(2.0)] for the respective catalytic yields. The zirconium sulfate precursor also leads to variations in catalytic activity of the supported catalysts with yields from 9.5 to 15.7%. On the other hand, catalytic yields for those synthesized with the chloride are higher than the former and bulk SZ and more similar to each other [catalytic yield: 28.4 and 24.9% for SZ/K-2(2.0) and SZ/K-2a(3.9), respectively].

3.6. Sulfating agent and sulfur contents

Catalytic yields differ only slightly for SZ/Si-2 series samples with yields between 4 and 7.5%, which makes it difficult to determine the influence of the sulfur contents on the catalytic activity. A comparison of the series catalysts, SZ/Si-2 and SZ/Al-2 (Table 3), shows that both systems adsorb sulfate effectively ($S_{theor.} = S_{exptl.}$) up to about 3.0 wt.% S with adsorption tapering off when $S_{theor.} > 3.0$ wt.% (Table 1). It seems both systems are not able to stabilize higher sulfur contents. The sulfur contents of the supported catalysts (18 wt.% S-based on ZrO_2) are much higher than that of unsupported SZ (usually <5.0 wt.% S [1,11–13,16,17], which was also observed in [5,6].

The samples, SZ/Al-2c(2.9) and SZ/Al-2d(3.3), show very low catalytic activity (catalytic yields: ≤1.1%); therefore, the series was not tested further catalytically. The γ-Al_2O_3 supported catalysts (SZ/Al-2a–e; Table 3) become inactive with increasing sulfur contents, when sulfated with H_2SO_4. This is probably due to the reaction of the support with H_2SO_4 to form $Al_2(SO_4)_3$ and is indicated by the lower intensity of the γ-Al_2O_3 peaks and absence of the ZrO_2 peak at 30° in the XRD pattern (Fig. 1c). In [6], the γ-Al_2O_3-supported catalysts were sulfated with $(NH_4)_2SO_4$ to avoid this problem. Sulfation with $(NH_4)_2SO_4$ did improve catalytic yields to 5.6 and 7.0%, for samples SZ/Al-od(2.2) and -fd(2.2), respectively. In the case of the inert SiO_2 support, sulfation was done exclusively with H_2SO_4 and is more effective and controllable: SZ/Si-2b(2.0) and SZ/Si-2b1(1.9) (Table 3).

4. Conclusions

In conclusion, the highest catalytic yields in the benzoylation of anisole were achieved with K-10-supported SZ catalysts. Yet, this catalytic activity is strongly affected by the ZrO_2 precursor used. Surface properties of the SZ are improved over that of bulk SZ with higher surface areas, pore volume, and pore diameter. However, the K-10-supported SZ catalyst with a low surface area, pore volume, and pore diameter, SZ/K-2(2.0), was the most active. Thus, the surface properties seem to play a secondary role in catalytic activity in comparison to other factors, such as acidity; this has been mentioned before [7]. The FTIR-PAS results agree with earlier reports on the main formation of PACs on Lewis acid sites in SZ/Al_2O_3 and SZ/SiO_2 [6,13]. Slight changes in the total number of acid sites of SZ/SiO_2 with the sulfur contents had no large effect on catalytic activity. This suggests that the number of acid sites (predominantly Lewis) in these samples is not conducive to catalytic activity. The sulfation of supported ZrO_2 results in little change in acid sites, for example, from Lewis acid sites to Brønsted acid sites, as in the case of bulk ZrO_2. However, catalytic activities higher than that of bulk SZ can be achieved with the use of a support providing Brønsted acid sites, such as K-10.

Acknowledgements

We would like to thank the Bundesministerium für Bildung und Forschung (BMBF) for financial support, Sigrid Bäßler for the acidity measurements, and Elfriede Lieske for the catalytic work.

References

[1] V. Quaschning, J. Deutsch, P. Druska, H.-J. Niclas, E. Kemnitz, J. Catal. 177 (1998) 164–174.
[2] G.A. Olah, Friedel–Crafts and Related Reactions, Wiley-Interscience, New York, 1963.
[3] G.D. Yadav, J.J. Nair, Micropor. Mater. 33 (1999) 1–48.
[4] S. Wang, J.A. Guin, Chem. Commun. (2000) 2499–2500.
[5] Y. Huang, B. Zhao, Y. Xie, Appl. Catal. A 173 (1998) 27–35.
[6] T. Lei, J.S. Xu, Y. Tang, W.M. Hua, Z. Gao, Appl. Catal. A 192 (2000) 181–188.
[7] H. Matsuhashi, M. Tanaka, H. Nakamura, K. Arata, Appl. Catal. A 201 (2001) 1–5.
[8] J.M. Grau, C.R. Vera, J.M. Parera, Appl. Catal. A 172 (1998) 311–326.
[9] S. Damyanova, P. Grange, B. Delmon, J. Catal. 168 (1997) 421–430.
[10] PDF-No. 19-0723, PCPDFWIN, Version 2.2, JCPDS-ICDD, June 2001. Reference: US Bureau of Mines, Open File Report.
[11] K. Parida, V. Quaschning, E. Lieske, E. Kemnitz, J. Mater. Chem. 11 (2001) 1903–1911.
[12] V. Quaschning, A. Auroux, J. Deutsch, H. Lieske, E. Kemnitz, J. Catal. 203 (2) (2001) 426–433.
[13] Y. Sun, L. Zhu, H. Lu, R. Wang, S. Lin, D. Jiang, F.S. Xiao, Appl. Catal. A 237 (2002) 21–31.
[14] J. Clark, S.R. Cullen, S.J. Barlow, T.W. Bastok, J. Chem. Soc., Perkin Trans. 2 (1994) 117–1131.
[15] R.J. Gorte, Catal. Today 28 (1996) 405–414.
[16] H.K. Mishra, K.M. Parida, Appl. Catal. A 224 (2002) 179–189.
[17] D.J. Zalewski, S. Alerasool, P.K. Doolin, Catal. Today 53 (1999) 419–432.